Archives of Hydro-Engineering and Environmental Mechanics
Vol. 54 (2007), No. 3, pp. 223–242

Grain Kinematics in Weak Linear Transport

Francesco Ballio, Alessio Radice

Politecnico di Milano, Dept. I.I.A.R., Piazza Leonardo da Vinci, 32, 20133 Milano, Italy,
e-mails: francesco.ballio@polimi.it, alessio.radice@polimi.it
Corresponding Author: Prof. Francesco Ballio

(Received September 25, 2007; revised November 07, 2007)

Abstract

Some preliminary results of measurements of one-dimensional sediment transport on a flat bed are presented. Image processing was applied to measure the time evolution of the areal concentration and the velocity of transported grains in a series of bed-load tests with values of the bed shear stress up to twice the threshold for incipient motion. The concentration and velocity data were used to compute the time evolution of the solid discharge per unit width. It was found, as expected, that the sediment transport is an episodic phenomenon, particularly at low shear stress; visualization of the moving particles allows recognition of the existence of longitudinal streaks, that can be more clearly observed when the sediment rate is weaker. The first and second order statistics of sediment concentration and velocity and solid discharge have been analyzed; the mean and standard deviation of the quantities increase as the transport intensity increases, while the coefficient of variation decreases. The ranges of variation of all the time-averaged quantities with the mean sediment rate are narrower if the zero values of the samples are disregarded prior to calculating the statistics; the coefficient of variation is almost constant. The solid discharge data samples were analyzed in the amplitude domain, by calculating the Cumulative Frequency Distributions; it was found that the shape of the CFDs computed with reference to the non-zero values of the sediment rate alone is self-similar regardless of the transport intensity.

Key words: sediment transport, grain concentration and velocity, solid discharge

Notation

The following symbols are used in this paper:

A	–	reference area for the measurement of sediment concentration and velocity,
B	–	constant of the logarithmic law of the wall,
C	–	sediment concentration,
$CV(X)$	–	coefficient of variation of the X quantity,
$CV(X)_{NZ}$	–	coefficient of variation of the X quantity with reference to the non-zero values,
d	–	duration of a sediment transport test,

d_{50} – median sediment diameter,
d_{90} – sediment diameter corresponding to the 90th percentile,
F – dimensionless sediment velocity,
g – gravity,
N – number of moving sediments for the measurement of concentration,
n – number of sediments passing over the plate,
Q – water discharge,
Q_c – threshold value of the water discharge,
q_s – longitudinal component of the solid discharge per unit width,
$\mathbf{q}_s$ – vector solid discharge per unit width,
q_{sp} – solid discharge measured at the plate,
t – time,
u – longitudinal component of the sediment velocity,
u^* – shear velocity,
u_c^* – threshold value of the shear velocity,
u_w – longitudinal water velocity,
$\mathbf{v}$ – vector sediment velocity,
w – width of the plate,
W_g – volume of one sediment particle,
z – elevation,
Δ – specific gravity of the sediments,
Φ – dimensionless solid discharge per unit width,
ϕ – Shields number,
ϕ_c – threshold value of the Shields number,
κ – Karman constant,
$\mu(X)$ – average value of the X quantity,
$\mu(X)_{NZ}$ – average value of the X quantity with reference to the non-zero values,
ν – kinematic viscosity of water.
ρ – density of water,
ρ_g – density of the sediments,
$\sigma(X)$ – standard deviation of the X quantity,
$\sigma(X)_{NZ}$ – standard deviation of the X quantity with reference to the non-zero values.

1. Introduction

The transport of sediments by a water stream in the proximity of a granular bed has been typically studied in order to develop reliable tools for the evaluation of the expected solid discharge for given flow conditions; pioneering work on this topic

was carried out in the 30s of the last century, for example by Shields, Einstein or Meyer-Peter and Mueller.

More recently, some researchers have paid attention to the behaviour of individual saltating particles (among others, Lee and Hsu (1994), Niño and Garcìa (1998), Ancey et al (2002), can be cited). Such characteristics as the height or length of individual jumps, as well as the fractions of rolling or saltating sediments, were analyzed in order to better describe the phenomenology of the particle motion at a scale comparable with the sediment size.

In recent years, sediment entrainment and motion have been related to events in the burst cycle within the turbulent boundary layer in the proximity of the bed (for a description of the features of the boundary layer on a rough bed, see for example (Grass 1971)). Nelson et al (1995) made simultaneous LDA measurements of the flow velocity in one point and of the solid discharge; by means of correlation analysis, they attributed the particle entrainment to the sweep events of the burst cycle. Sechet and Le Guennec (1999) made LDA single-point measurements of the flow velocity and particle tracking of the entrained solid particles around threshold conditions; they compared the characteristic time scales of ejection events and those of the sediment motion, finding a good correlation. Other works focused only on the sediment motion: Drake et al (1988), while analyzing the bed load in a field case, attributed most of the sediment motion to 'sweep transport events' of particular strength. Niño and Garcìa (1996) analyzed the almost suspended motion of sediments and indicated a link between the sediment entrainment and ejection events. It can be seen that encouraging indications have been obtained thanks to similar approaches, yet the available literature studies are still too scarce to set up a comprehensive framework.

The precedent considerations suggest that observation of the phenomenology of the sediment transport on a plane bed may help understanding of the process on a small scale. Although such characterization may be too refined with respect to engineering problems in a one-dimensional case, it is needed for the understanding of more complex cases, that can differ from the one-dimensional one (Nelson et al 1995). In this work, some preliminary observations on the phenomenology of the bed load will be made, with reference to weak sediment transport conditions. Results of measurements of the concentration and velocity of the moving particles will be documented.

2. Experimental Setup and Procedure

2.1. Flume Facility

The experiments reported herein have been performed in a pressurized rectangular duct with transparent walls; the duct length is equal to 5.8 m, the cross section is 40 cm wide and 16 cm deep. The hydraulic head in the duct is imposed by a weir

located in the downstream tank; the upstream tank is provided with a streamlined inlet to avoid wakes in the flow.

The test reach of the duct is 2 m long, starting at approximately 2.6 m from the inlet. Two different channel modules are available: for experiments with a fixed bed a module with a height of 16 cm is used, while for the experiments with a movable bed a deeper module is used. The latter was filled with plastic sediments having a specific gravity $\Delta = (\rho_g - \rho)/\rho = 0.43$, with ρ_g and ρ being the densities of sediments and water, respectively. The sediments are almost uniform: the median diameter is $d_{50} = 3.6$ mm, while the diameter corresponding to the 90^{th} percent has been estimated as $d_{90} = 3.73$ mm. The latter was used as the representative bed roughness. In all the duct modules with small depth, the same roughness was obtained by gluing the same sediments onto metallic sheets located on the bottom wall of the duct.

Water discharge has been measured by a magnetic flowmeter mounted on the delivery pipe. All the remaining measurements have been made by image processing: to capture moving pictures a black and white CCD camera has been used, with a sampling frequency of 50 Hz.

2.2. Incipient Motion and Bed Shear Stress

The incipient motion of bed particles is not a well defined phenomenological condition, and therefore it is not possible to define a sharp threshold for sediment motion (see, for example, Grass 1970, Buffington 1999, Shvidchenko and Pender 2000). We defined incipient motion as the condition corresponding to a given weak sediment transport: in particular, we define the dimensionless solid discharge per unit width as:

$$\Phi = \frac{q_s}{\sqrt{g \cdot \Delta \cdot d_{50}^3}}, \tag{1}$$

where q_s is the solid discharge per unit width and g is gravity; furthermore, we identify the threshold conditions with $\Phi = 5.7 \cdot 10^{-5}$. The threshold water discharge was determined during experimental tests with very weak sediment transport, in which the sediment rate was measured by counting the grains passing over a plate used as a sight; the unit width solid discharge over the plate for each test was calculated as:

$$q_{sp} = \frac{n \cdot W_g}{d \cdot w}, \tag{2}$$

where n is the number of grains passed over the plate, W_g is the volume of a single grain, d is the test duration and w is the plate width. The threshold water discharge was $Q_c = 18.95$ l/s.

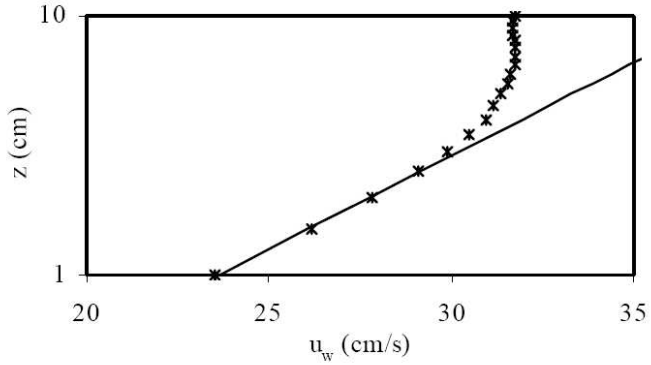

Fig. 1. Fit of the log law to the near-bed velocity profile in the channel axis

The shear velocity at the granular bed (hereafter indicated with u^*) was evaluated through the vertical distribution of the flow velocity in an experiment with a fixed bed and a discharge of Q = 17.9 l/s. The water velocity profile was measured in the channel axis. A Particle Tracking Velocimetry algorithm (see Malavasi et al 2004) was applied to movies captured after seeding the current with neutrally buoyant polystyrene particles of 400 μm in size. The time-averaged velocity profile in the proximity of the bed is shown in Fig. 1; a logarithmic law of the wall was fitted to the experimental data in the form:

$$\frac{u_w(z)}{u^*} = \frac{1}{\kappa} \ln \frac{z}{d_{90}} + B, \tag{3}$$

where u_w is the water velocity at a certain z level and κ is the von Karman constant, that we assumed equal to 0.41. For the test with Q = 17.9 l/s we found a shear velocity u^* = 2.46 cm/s and a 7.2 value for the constant B from the velocity profile. The ratio Q/Q_c was assumed to be equal to the ratio u^*/u_c^*, since no significant bed forms occurred in our experiments. It is worth clarifying that our shear velocity is a measure of only the skin friction (grain-related) shear stress, which is indeed the effective shear stress for the solid discharge. The critical value of the shear velocity u_c^* was therefore equal to 2.60 cm/s.

In the bed load tests documented here, the water discharge Q was measured and therefore the ratio Q/Q_c was computed. The shear velocity was calculated as $u^* = u_c^* \cdot Q/Q_c$. The water discharge ranged from 19.8 to 27.5 l/s, and the corresponding average water velocity varied from 0.32 to 0.44 m/s. As a result, the shear velocity ratio u^*/u_c^* in our experimental tests varies from 1.04 to 1.45.

2.3. Measurement of the Sediment Motion

The concentration and velocity of the moving grains have been measured by image processing in the region upstream of the plate. Radice et al (2006) devised a method for the automatic measurement of the instantaneous values of the quantities of interest: the measurement of the concentration is based on the subtraction of consecutive frames and following filtering procedures for the recognition of the moving particles; the measurement of sediment velocity is based on Particle Image Velocimetry applied to images obtained again by subtracting consecutive frames. All the measurements are referred to a certain support area A, the dimension of which equals that of some tens of grains. Under weak sediment transport, the depth of the active sediment layer equals the particle dimension, and the instantaneous values of the vector unit width solid discharge can be calculated as:

$$\mathbf{q}_s = C \cdot \mathbf{v} \cdot d_{50}, \tag{4}$$

where C is the areal concentration of the moving sediments and $\mathbf{v}$ is the sediment velocity (the longitudinal component of which will be denoted by u). The sediment concentration is defined as:

$$C = \frac{N \cdot W_g}{A \cdot d_{50}}, \tag{5}$$

where N is the number of grains moving over the measuring area A.

Radice et al (2006) showed that image processing is very powerful in measuring instantaneous values of the quantities of interest, but the parameters of the processing algorithms have to be determined via a calibration of the measuring method against given solid discharge values. In this work, the films of the transport experiments have been manually post-processed and the number of the sediments crossing the plate during each test has been determined; the average sediment rate has then been evaluated by equation (2). On the other hand, the temporal series of the solid discharge automatically given by the image processing through equation (4) have been averaged in order to obtain values to be compared to the real ones, coming from the direct count of the grains. The comparison between the real values and those obtained by the measuring technique is presented in Fig. 2; both sediment rates are made dimensionless by equation (1). The values of the solid discharge from image processing are in good agreement with the real ones. Sediment transport rates varying within two orders of magnitude are correctly measured, except for a visible underestimation of the sediment flux for very low solid discharges. Such behaviour is analogous to that found by Radice et al (2006) when measuring the solid discharge of natural sand.

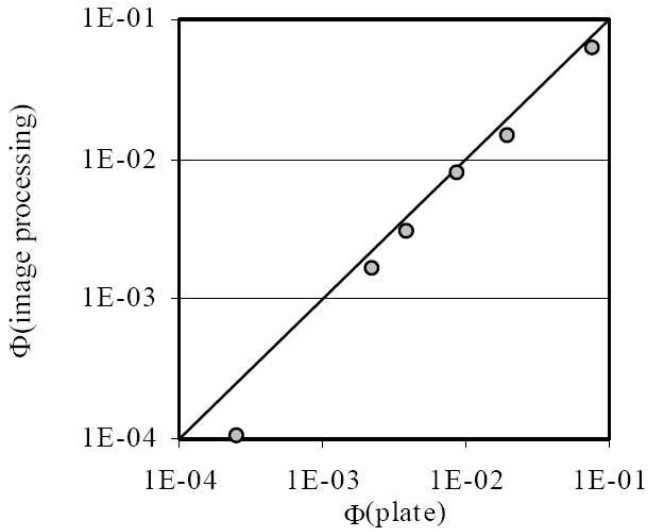

Fig. 2. Verification of the reliability of the average values measured for the sediment rate

3. Experimental Results on Particle Motion

Fig. 3 depicts the temporal evolution of the sediment concentration and velocity and of the solid discharge per unit width for the condition $u^*/u_c^* = 1.41$. The dimensionless sediment velocity is defined as:

$$F = \frac{u}{\sqrt{g \cdot \Delta \cdot d_{50}}}; \tag{6}$$

given equation (1) for the dimensionless solid discharge, the longitudinal component of equation (4) becomes:

$$\Phi = C \cdot F. \tag{7}$$

All the quantities fluctuate in time. Similar successions of crests and troughs can be observed for concentration and solid discharge, with the relative height of the peaks being determined by the values of the sediment velocity. Even if the normalization of the quantities makes it difficult to see it from the plots, mean values of the sediment velocity are of the same order of magnitude as the shear velocity, while peak values are almost equal to the average velocity of the flow. In some instants the quantities are equal to zero, indicating that no motion occurred in that instant at the location investigated.

The same quantities are plotted for a different transport condition ($u^*/u_c^* = 1.31$) in Fig. 4. The curves presented are qualitatively similar to the previous ones, but the number of instants where no motion was detected is visibly larger than for the

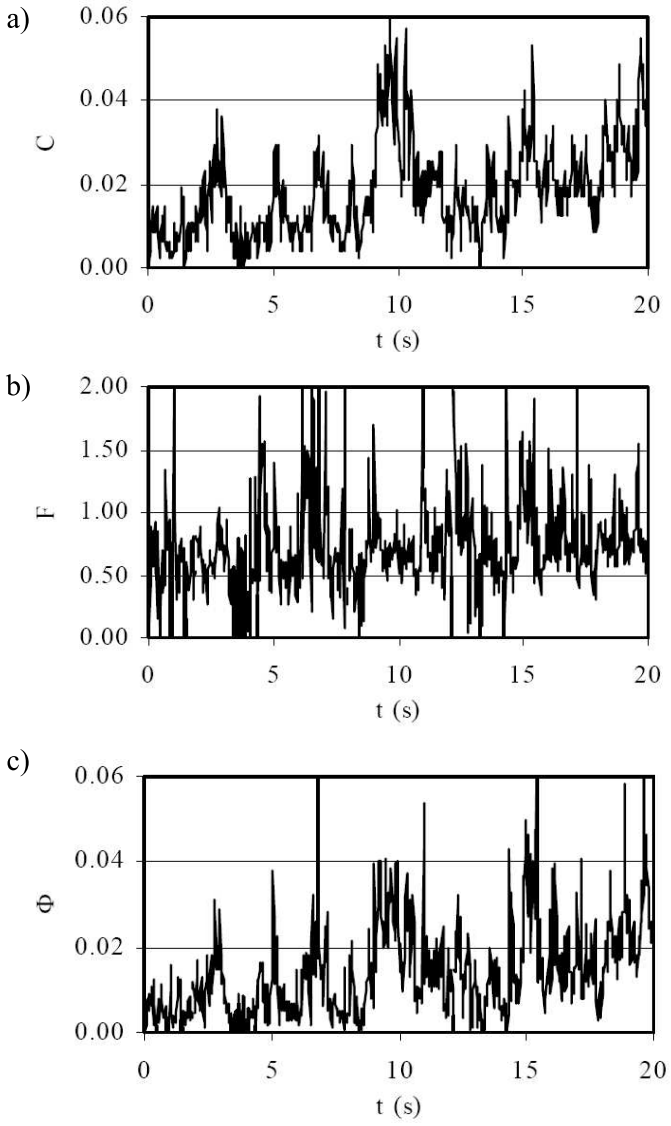

Fig. 3. Temporal series of the concentration (a), longitudinal velocity (b), longitudinal solid discharge per unit width (c). Test 5, $u^*/u^*c = 1.41$

previous transport condition. The increase of the relative stillness of the grains is evident, if we consider the transport conditions just above the incipient motion, depicted in Fig. 5. Radice and Ballio (2007) defined an intermittency factor as the percentage of stillness of the sediments in a measuring area within a time series, and showed that indeed the value of this factor varies from almost unity close to the incipient motion to zero for shear stresses of almost twice the threshold value.

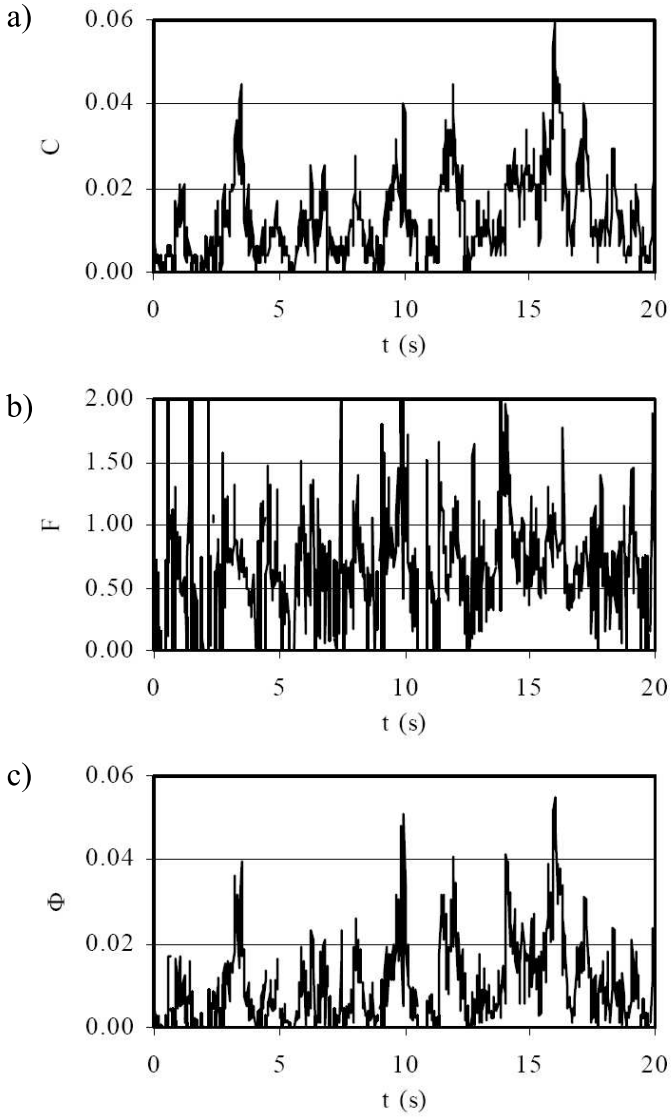

Fig. 4. Temporal series of the concentration (a), longitudinal velocity (b), longitudinal solid discharge per unit width (c). Test 3, $u^*/u^*c = 1.31$

It is reported in the literature that the motion of sediments on a granular bed is organized in longitudinal streaks, which are the trace of the existence of lateral structures in the turbulent boundary layer close to the bed; similar structures have been observed, for example, by Grass (1971) and by Niño and Garcìa (1996), who affirmed that the particle streaks are of a width of about 100 wall units for hydraulically smooth flows (the wall length scale is defined as ν/u^*, where ν is the

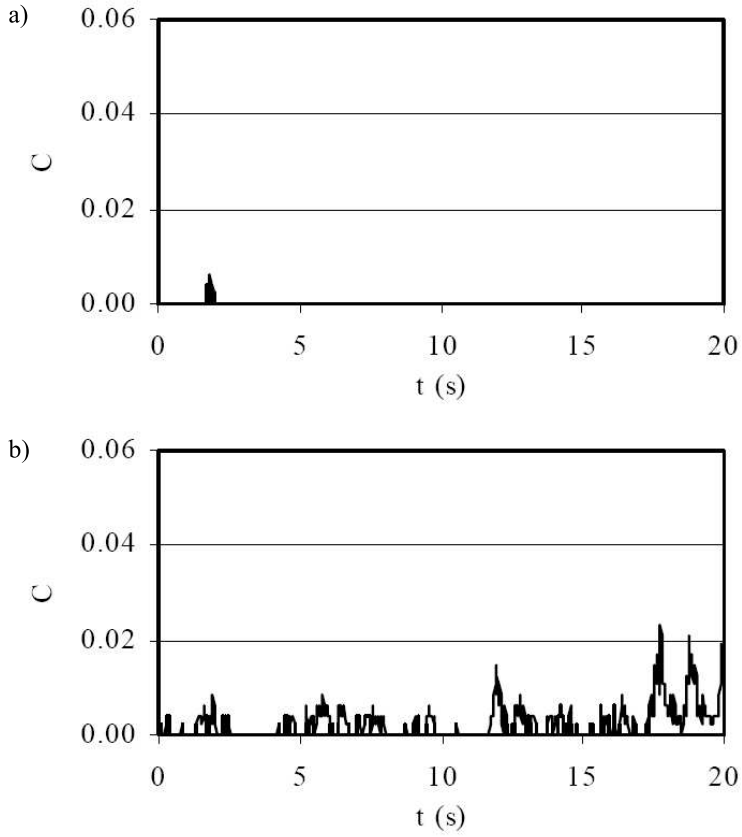

Fig. 5. Temporal series of the concentration: (a) test 1 (u^*/u^*c = 1.04) and (b) test 4 (u^*/u^*c = 1.11)

kinematic viscosity of water). We have visualized the moving sediments by computing the difference between consecutive frames of the movies and accumulating images. Fig. 6 depicts two examples of visualization for the experiment with u^*/u_c^* = 1.11. Two streaks can be recognized, with a width corresponding to about 10–20 particle sizes. The spatial pattern of the streaks varies in time, since the streaks do not always occur in the same position; therefore, the accumulation of the images must be done with reference to a short time period in order to avoid accumulation of the grains in all the area investigated. Figs. 7 and 8 present similar visualizations for u^*/u_c^* = 1.31 and u^*/u_c^* = 1.45, respectively. As the shear stress is increased and the intensity of sediment motion rises correspondingly, the streaks are much less recognizable, even for accumulation periods that are considerably shorter than for the previous case. In synthesis, the existence of the particle streaks seems to be confirmed by present experimental findings, but they are clearly observed only for very low transport conditions.

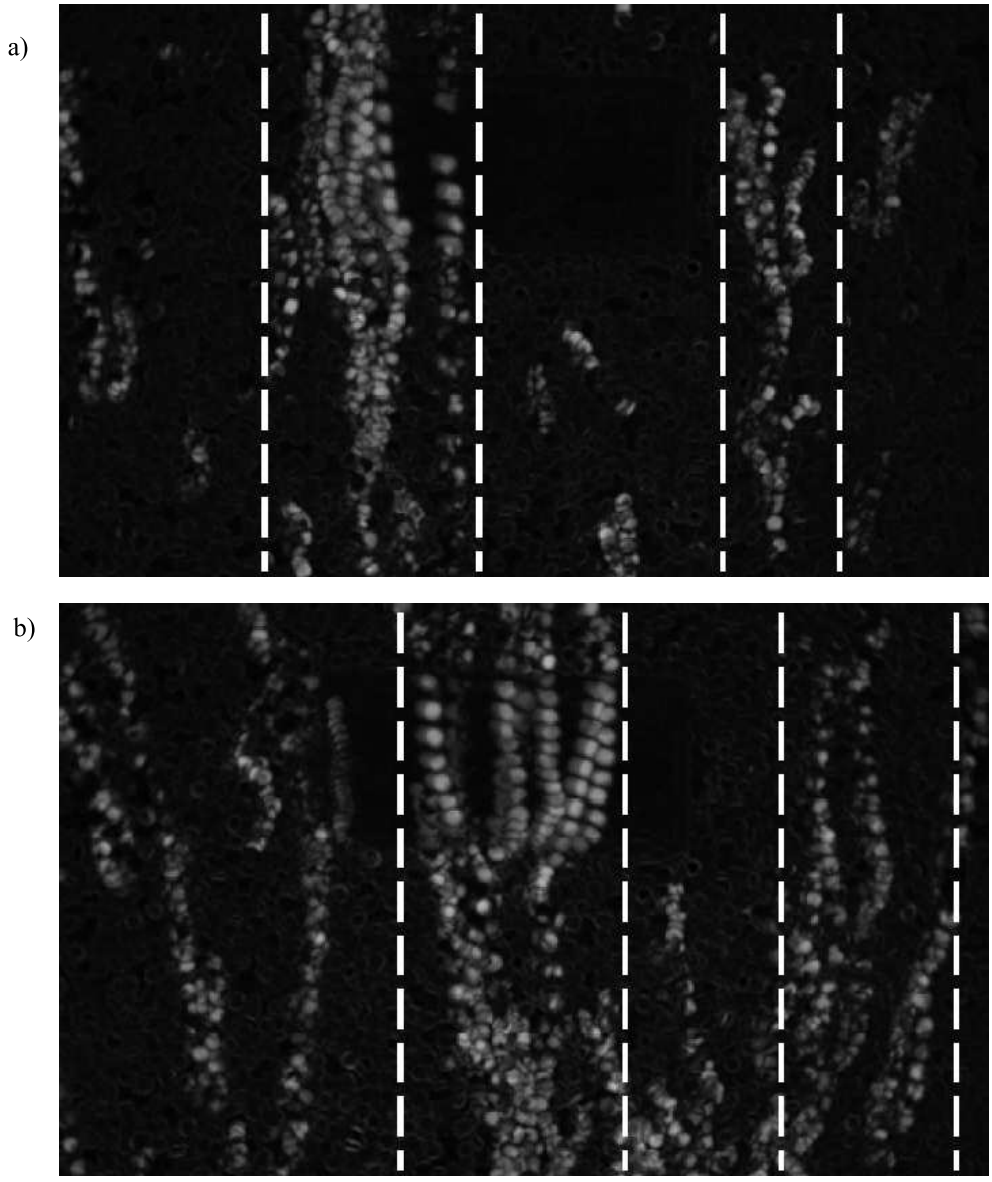

Fig. 6. Visualizations of the sediment streaks for two different periods during test 4 (u^*/u^*c = 1.11). The temporal interval for the accumulation of the particle images is 0.8 s for both (a) and (b). The sediment streaks are highlighted through the dashed lines

The temporal series of each measured quantity were averaged in order to compare the measured mean values with previous literature results. The variation of the areal concentration of moving sediments with the shear stress was compared with the equations proposed by Fernandez Luque and Van Beek (1976) and by Van Rijn (1984). The structure of the Van Rijn equation refers to a depth averaged

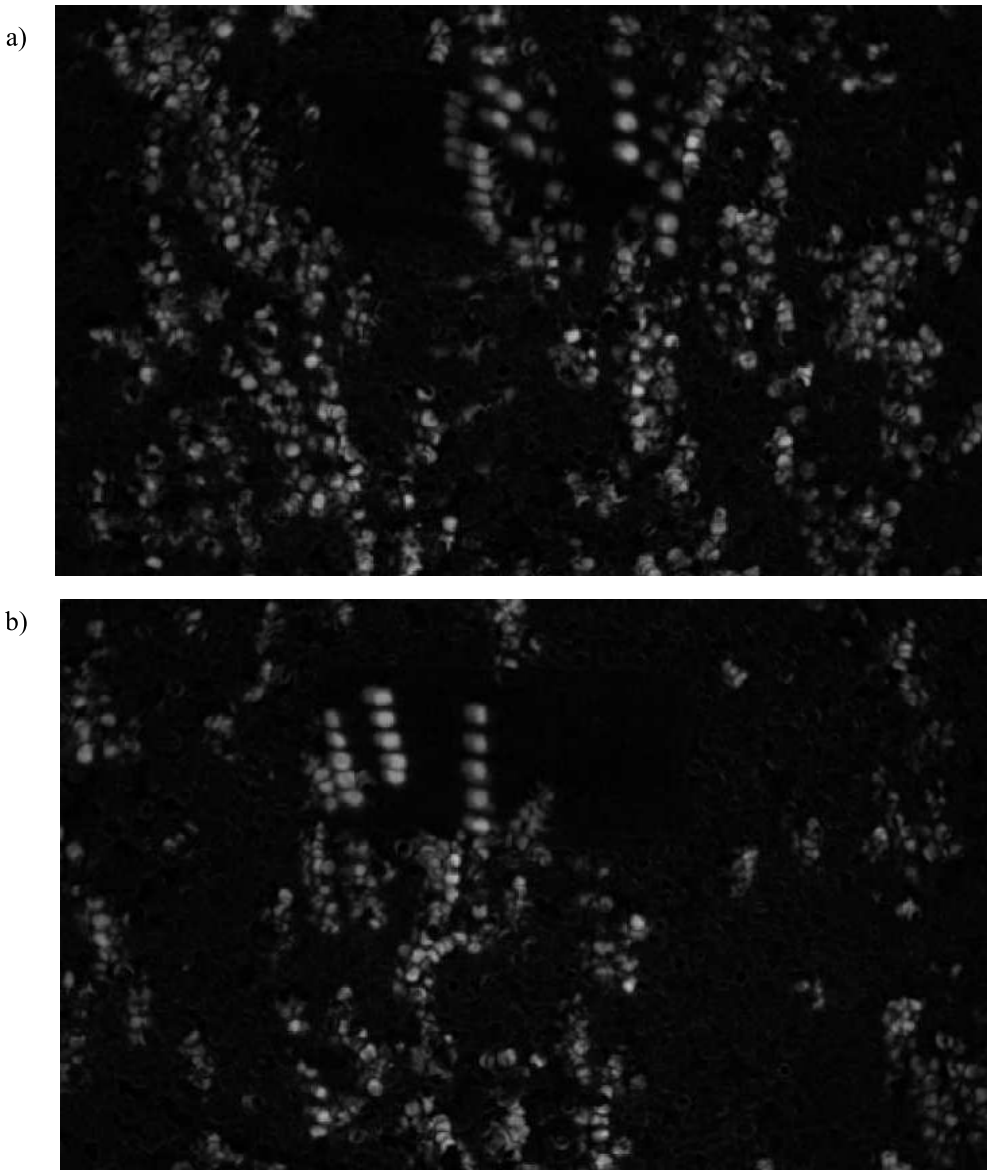

Fig. 7. Visualizations of the sediment streaks for two different periods during test 3 (u^*/u^*c = 1.31). The temporal interval for the accumulation of the particle images is 0.08 s for both (a) and (b)

approach: the solid discharge is calculated as $q_s = C_s \cdot \delta_s \cdot v_s$, where C_s is the depth averaged concentration in a bed load layer where saltation height is δ_s, and v_s is particle velocity; a comparison with equation (4) indicates that our areal concentration must be compared with the quantity $C_s \cdot \delta_s/d_{50}$. The comparison is presented in Fig. 9. The same figure shows the variation of the dimensionless unit width solid

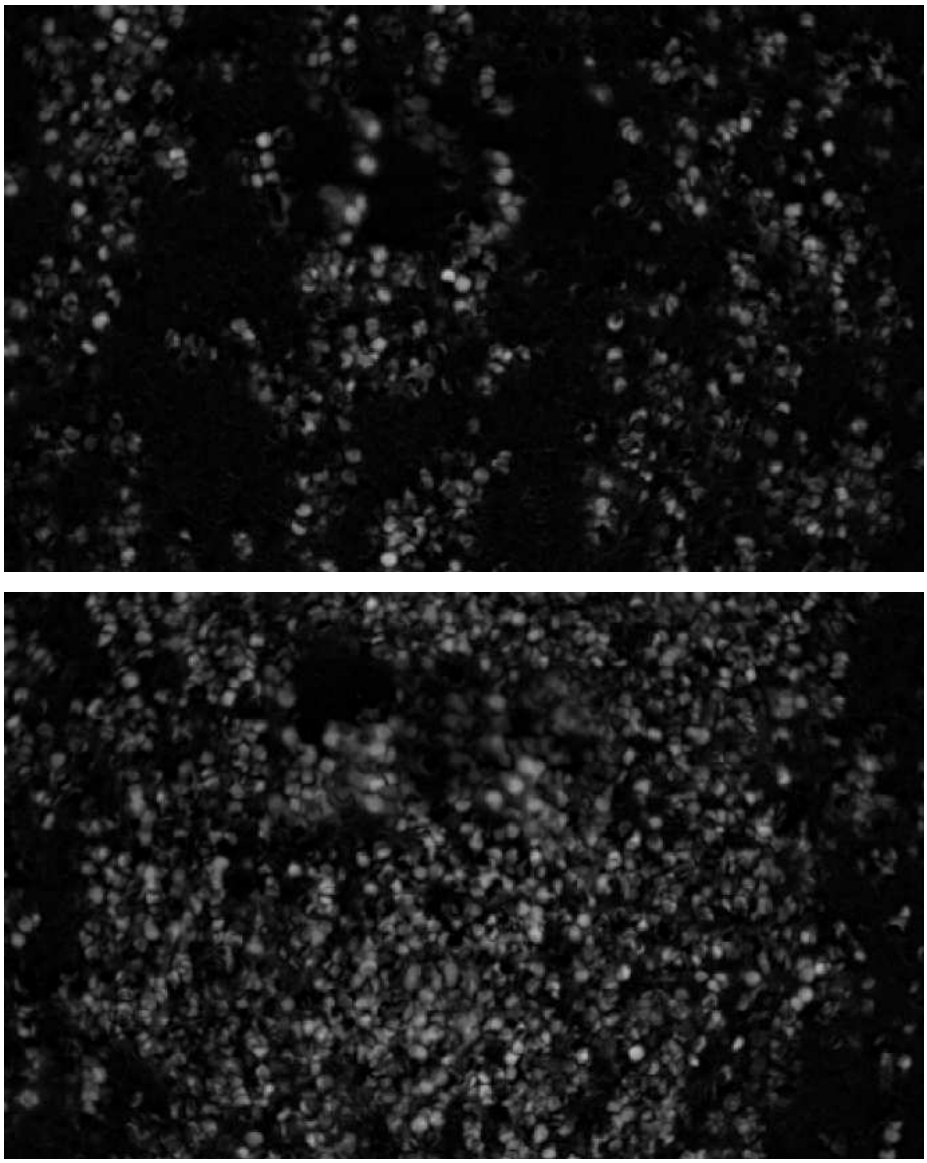

Fig. 8. Visualizations of the sediment streaks for two different periods during test 6 (u^*/u^*c = 1.45). The temporal interval for the accumulation of the particle images is 0.04 s for both (a) and (b)

discharge with the shear stress, compared with the equations of Meyer-Peter and Mueller (1948) and Van Rijn (1984). For the concentration values, the literature equations spread over an order of magnitude; our data lay within the corresponding range. For the solid discharge values, our tests are in closer agreement with the

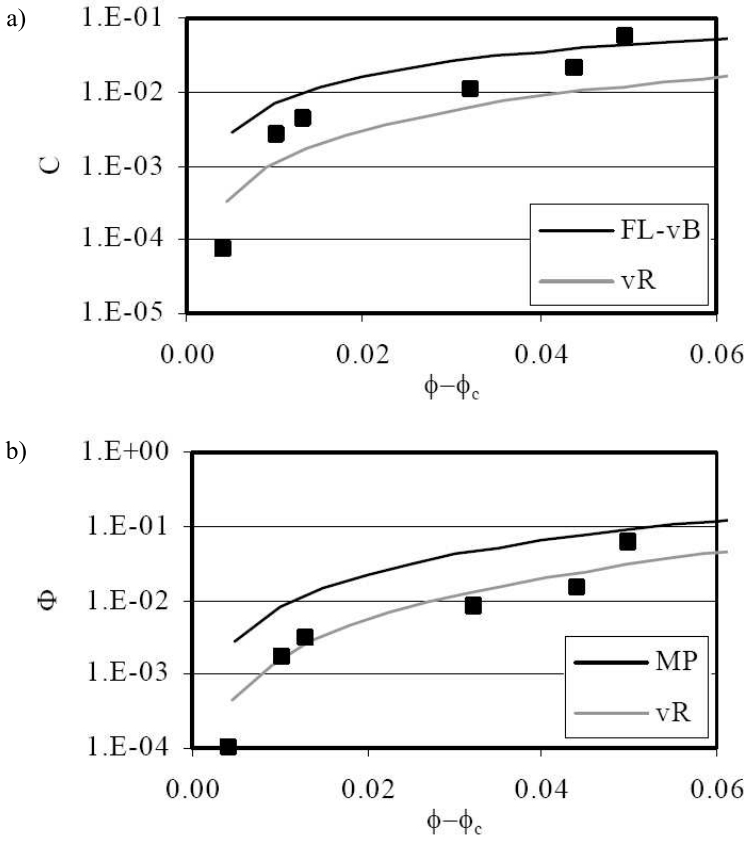

Fig. 9. Fit to the experimental data of the literature formulas for the prediction of sediment concentration (a) and solid discharge (b). In the legend, FL-vB represents Fernandez Luque and Van Beek (1976); vR represents Van Rijn (1984); MP represents Meyer-Peter and Mueller (1948)

equation of Van Rijn (1984). The agreement between the measured data and the equation by Meyer-Peter and Mueller increases with the shear stress.

4. Statistical Analysis of the Measured Quantities

The temporal series of all the measured quantities were averaged. The second-order statistics have also been calculated: the standard deviation of the samples and the coefficient of variation CV, intended as the standard deviation normalized over the mean. As previously recalled, Radice and Ballio (2007) showed that the intermittency of the sediment motion plays a considerable role in determining the resulting average values of the sediment transport rate, and that most of the variability of the sediment transport can be interpreted by removing the intermittency and considering data samples with only the non-zero values of the quantities. Therefore, we

performed our statistical analyses with reference to both the original data samples and those with only the non-zero values. We indicate with $\mu(X)$, $\sigma(X)$ and $CV(X)$ the mean, the standard deviation and the coefficient of variation of X quantity, respectively, with reference to the original data samples. We denote by $\mu(X)_{NZ}$, $\sigma(X)_{NZ}$ and $CV(X)_{NZ}$ the same statistical parameters with reference to the samples of the non-zero values.

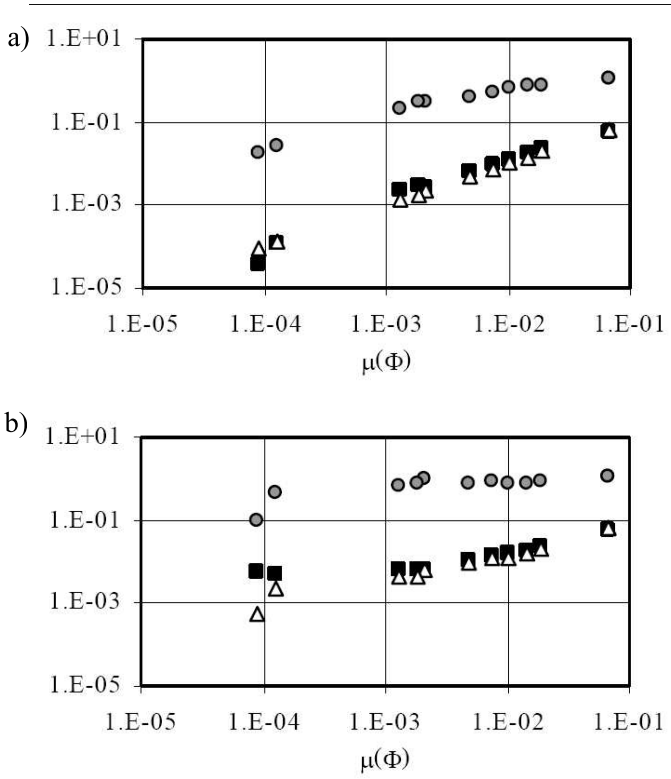

Fig. 10. Time-averaged values of the quantities. All the values (a) and non-zero values (b). Symbols: ■, sediment concentration, $\mu(C)$ or $\mu(C)_{NZ}$; ○, sediment velocity, $\mu(F)$ or $\mu(F)_{NZ}$; △, solid discharge per unit width, $\mu(\Phi)$ or $\mu(\Phi)_{NZ}$

The correlation between the time-averaged values of the quantities is depicted in Fig. 10. The quantities are obviously correlated; it is, however, interesting that, for the same variation of the shear stress, concentration and solid discharge values vary by more than three orders of magnitude, whereas velocity values vary by only two orders of magnitude, indicating that, whatever the reason of the sediment motion, it influences the concentration more than the sediment velocity. After removing the zero values, the means of the quantities typically increase, the growth being larger for the experiments with lower shear stress where the effect of the intermittency is higher; in consequence, all the ranges of variation of the quantities become

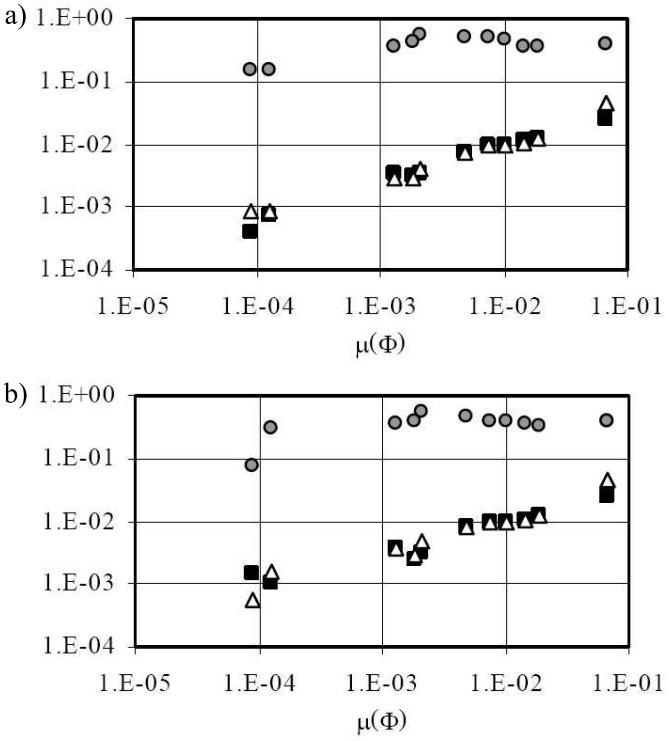

Fig. 11. Standard deviation of the data samples for the quantities. All the values (a) and non-zero values (b). Symbols: ■, sediment concentration, $\sigma(C)$ or $\sigma(C)_{NZ}$; ●, sediment velocity, $\sigma(F)$ or $\sigma(F)_{NZ}$; △, solid discharge per unit width, $\sigma(\Phi)$ or $\sigma(\Phi)_{NZ}$

narrower. The minimum value of the non-zero sediment concentration is bounded by the condition corresponding to just one moving particle. It is also interesting to note that the non-zero time-averaged velocity varies very little. This is the actual velocity of the moving particles, whereas the total average is the effective velocity that accounts for the periods of rest between one entrainment and the following; we found the physical velocity of the particles being proportional to the shear velocity, in agreement with previous works (see the synthesis made by Niño and Garcìa 1998).

The standard deviation is presented in Fig. 11. Values for the concentration and the solid discharge exhibit a very similar behaviour, whereas the standard deviation of the velocity is less variable. When removing the zero values, the standard deviation of the samples varies very little. The distributions of the data within the samples of the solid discharge will be discussed in more detail afterwards.

The coefficient of variation (i.e. the ratio between the standard deviation and the mean) is depicted in Fig. 12. The *CV* decreases for all the quantities; furthermore, the values of this coefficient for the three quantities are all very similar. Finally,

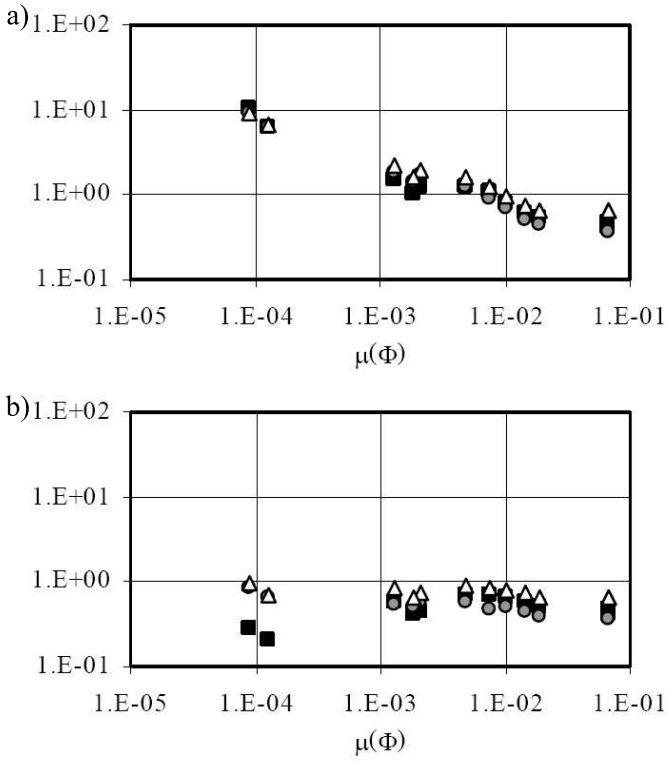

Fig. 12. Coefficient of variation of the data samples for the quantities. All the values (a) and non-zero values (b). Symbols: ■, sediment concentration, $CV(C)$ or $CV(C)_{NZ}$; ◎, sediment velocity, $CV(F)$ or $CV(F)_{NZ}$; △, solid discharge per unit width, $CV(\Phi)$ or $CV(\Phi)_{NZ}$

when removing the zeros, the range of variation of this coefficient decreases from 1.5 orders of magnitude to half an order of magnitude, indicating again that much of the variability of the quantities is related to the intermittency of the sediment motion.

We have analyzed the data samples of the solid discharge in the amplitude domain. The Cumulative Frequency Distributions obtained are shown in Fig. 13. Sediment rates (x-axis of the plots) are normalized by their mean values, so that the shapes of the distributions can be compared. For the curves computed with the entire data samples (Fig. 13a) the intersection with the y-axis represents the percentage of zero values, which, as already discussed, decreases with increasing transport intensities. For the largest intensities, the percentage of zeros is negligible, and the normalized CFDs are coincident. Note that the absolute distributions do not coincide, as their means increase with the transport rate. The striking feature is that when we remove the zero values (Fig. 13b) the normalized distribution of the sediment rates is similar for all the transport conditions experimented. This last finding means that, whatever the average sediment transport rate is, the distribution

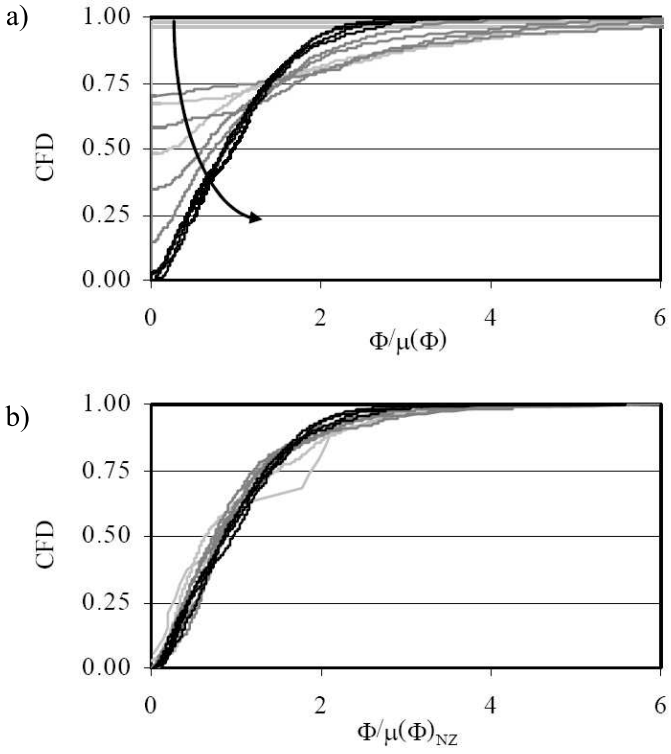

Fig. 13. Cumulated Frequency Distribution of the solid discharge for all the values (a, with the arrow indicating the growth of the shear velocity) and for the non-zero values (b)

of the transport events around the mean is always the same. This preliminary result should be verified with reference to a wider experimental campaign in which different sediments are used.

5. Conclusions

The major conclusions of this work are sketched in the following.

1. The sediment transport is an episodic phenomenon, particularly at shear stresses just above those corresponding to the threshold for the sediment motion. The temporal persistence of the particle motion increases with the shear stress. The time variation of the primitive quantities that concur in the determination of the solid discharge presents a similar succession of crests and troughs.

2. Visualization of the moving grains allows observing that the particle motion is organized in longitudinal streaks of a width of about 10–20 particle sizes. The streaks are most clearly observed for the weakest transport conditions.

3. As the bed shear stress is increased (and the average sediment transport rate is increased consequently) all the time-averaged values of the quantities increase; neglecting the zero values makes the ranges of variation narrower, and in particular, the physical velocity of the particles turns out to be directly proportional to the shear velocity. The irregularity of the sediment motion, expressed by the coefficient of variation, decreases as the sediment rate is larger; again, it is less variable when considering only the non-zero values. The standard deviation has an intermediate behaviour, in that it is a measure of the irregularity of the samples but it is also correlated with the mean.
4. The Cumulative Frequency Distribution of the solid discharge values is dominated by the zero values at very low shear stress. For growing stress, the zero values tend to vanish and the distributions tend to become similar. The distributions computed after removing the zero values are all similar, regardless of the average transport intensity.

References

Ancey C., Bigillon F., Frey P., Lanier J., Ducret R. (2002) Saltating motion of a bead in a rapid water stream, *Physical Review E*, **66**, 036306.

Buffington J. M. (1999) The legend of A. F. Shields, *Journal of Hydraulic Engineering*, **125** (4), 376–387.

Drake T. G., Shreve R. L., Dietrich W. E., Whiting P. J., Leopold L. B. (1988) Bedload transport of fine gravel observed by motion-picture photography, *Journal of Fluid Mechanics*, **192**, 193–217.

Fernandez Luque R., Van Beek R. (1976) Erosion and transport of bed-load sediment, *Journal of Hydraulic Research*, **14** (2), 127–144.

Grass A. J. (1970), Initial instability of fine bed sand, *Journal of the Hydraulics Division*, **96** (HY3), 619–632.

Grass A. J. (1971) Structural features of turbulent flow over smooth and rough boundaries, *Journal of Fluid Mechanics*, **50**, 233–255.

Lee H. Y., Hsu I. S. (1994) Investigation of saltating particle motions, *Journal of Hydraulic Engineering*, **120** (7), 831–845.

Malavasi S., Franzetti S., Blois G. (2004) PIV investigation of flow around submerged river bridge deck, *River Flow 2004, II Int. Conf. on Fluvial Hydraulics*, Naples, Italy, 1, 601–608.

Meyer-Peter E., Mueller R. (1948) Formulas for bed-load transport, *II Congress of IAHR*, Stockholm, Sweden.

Nelson J. M., Shreve R. L., McLean S. R., Drake T. G. (1995) Role of near-bed turbulence structure in bed load transport and bed form mechanics, *Water Resources Research*, **31** (8), 2071–2086.

Niño Y., Garcìa M. H. (1996) Experiments on particle-turbulence interactions in the near-wall region of an open channel flow: implications for sediment transport, *Journal of Fluid Mechanics*, **326**, 285–319.

Niño Y., Garcìa M. H. (1998) Experiments on saltation of sand in water, *Journal of Hydraulic Engineering*, **124** (10), 1014–1025.

Radice A., Ballio F. (2007) Average characteristics of sediment motion in one-dimensional bed load, *Acta Geophysica*, submitted.

Radice A., Malavasi S., Ballio F. (2006) Solid transport measurements through image processing, *Experiments in Fluids*, doi: 10.1007/s00348-006-0195-9.

Sechet P., Le Guennec B. (1999) Bursting phenomenon and incipient motion of solid particles in bed-load transport, *Journal of Hydraulic Research*, **37** (5), 683–696.

Shvidchenko A. B., Pender G. (2000) Initial motion of streambeds composed of coarse uniform sediments, *Proc. Inst. Civ. Eng., Water & Maritime Engng*, 142, 217–227.

Van Rijn L. C. (1984) Sediment transport, Part I: bed load transport, *Journal of Hydraulic Engineering*, **110** (10), 1431–1456.